JOURNAL OF GUIDANCE, CONTROL, AND DYNAMICS
Vol. 32, No. 4, July–August 2009

Engineering Notes

Optimal Orbital Rendezvous Maneuvering for Angles-Only Navigation

David C. Woffinden*
Charles Stark Draper Laboratory, Inc., Houston, Texas 77058
and
David K. Geller†
Utah State University, Logan, Utah 84322

DOI: 10.2514/1.45006

I. Introduction

ANGLES-ONLY navigation has great potential for orbital rendezvous, satellite formation flight, and other relative motion applications, but is often discarded because of its inherent and misunderstood limitation in determining range. A common consensus in the published literature, regardless of the application, is that maneuvers are generally required to obtain target observability when using only angle measurements [1–6]. For the bearings-only tracking problem, Nardone and Aidala [7] and Hepner and Geering [8] also showed that certain types of maneuvers, particularly those maneuvers that cause position changes that lie along the instantaneous bearing lines associated with a constant velocity trajectory, do not necessarily guarantee observability. If certain maneuvers produce observability and others do not, then the next natural step that has received considerable attention is to determine which maneuvers and trajectories are optimal in maximizing observability [9–16]. Despite these significant advances in deriving optimal maneuvers for the bearings-only tracking problem, these results are typically established on the premise of a constant moving target, an assumption valid for many naval applications that motivated the earlier research efforts but not applicable to orbital rendezvous. Although the influence of maneuvering for angles-only navigation has been considered for orbital rendezvous [17–19], there does not exist in the published literature derivations of performing optimal maneuvers to maximize observability. This Note develops the mathematical framework to analytically derive optimal maneuvers for angles-only navigation using a previously derived observability criteria [20–22]. The concept of having *levels* or *degrees* of observability is formally defined as a function of the measurement error and then used to form the theoretical foundation to derive optimal maneuvers that maximize the observability of the relative state. A simple yet common orbital rendezvous example is provided to illustrate the possibility of designing optimal orbital rendezvous maneuvers for angles-only navigation. Although the topic is introduced in the context of orbital rendezvous, the fundamental concepts can be applied to any linear dynamic system (and extended to nonlinear systems) for which the relative position and velocity are estimated using only angular measurements.

Received 16 April 2009; accepted for publication 18 April 2009.

*Senior Member of the Technical Staff; dwoffinden@draper.com.
†Assistant Professor, Mechanical and Aerospace Engineering; dgeller@engineering.usu.edu.

II. Relative Orbital Motion

The equations of motion describing the relative orbital dynamics between two or more spacecraft is commonly known as the Clohesy–Wiltshire (CW) or Hill's equations [23]. In terms of a dimensionless time quantity, $\tau = \omega t$, the CW equations can be expressed in a form that is independent of the orbital angular rate:

$$\begin{bmatrix} x'' \\ y'' \\ z'' \end{bmatrix} = \begin{bmatrix} -2z' \\ -y \\ 3z + 2x' \end{bmatrix} + \begin{bmatrix} a_x \\ a_y \\ a_z \end{bmatrix} \tag{1}$$

where x, y, and z are the components of the relative position vector in the local-vertical–local-horizontal coordinate system, and a_x, a_y, and a_z represent accelerations due to external forces, including the higher-order gravitational terms neglected in the linearized model. The x axis or downrange component is the *local horizontal* generally pointing along the target's velocity vector, the y axis or cross track is normal to the orbiting reference plane aligned with the orbital angular velocity $\boldsymbol{\omega}$, and the z axis or altitude is the *local vertical* pointing radially upward. The derivative operator is defined as $()' = \mathrm{d}()/\mathrm{d}\tau = (1/\omega)\mathrm{d}()/\mathrm{d}t$. The dimensionless CW equations formulated in Eq. (1) can also be written in state-space form $\boldsymbol{x}' = \boldsymbol{A}\boldsymbol{x} + \boldsymbol{B}\boldsymbol{u}$, where $\boldsymbol{x}(\tau) = [\boldsymbol{r} \quad \boldsymbol{v}] = [x \quad y \quad z \quad x' \quad y' \quad z']$ and the control input $\boldsymbol{u}$ represents the accelerations $\boldsymbol{a}(\tau)$. The solution to this well-known differential equation is

$$\boldsymbol{x}(\tau) = \boldsymbol{\Phi}(\tau, \tau_0)\boldsymbol{x}(\tau_0) + \int_{\tau_0}^{\tau} \boldsymbol{\Phi}(\tau, \mu)\boldsymbol{B}\boldsymbol{a}(\mu)\,\mathrm{d}\mu \tag{2}$$

where state transition matrix $\boldsymbol{\Phi}(\tau, \tau_0) = e^{\boldsymbol{A}(\tau - \tau_0)}$ can be expressed with the shorthand notation $\Delta\tau_0 = \tau - \tau_0$, $\tau_0 = \omega t_0$, $s_0 = \sin(\Delta\tau_0)$, and $c_0 = \cos(\Delta\tau_0)$.

$$\boldsymbol{\Phi}(\tau, \tau_0) = \begin{bmatrix} \boldsymbol{\Phi}_{rr} & \boldsymbol{\Phi}_{rv} \\ \boldsymbol{\Phi}_{vr} & \boldsymbol{\Phi}_{vv} \end{bmatrix} = \begin{bmatrix} 1 & 0 & 6(s_0 - \Delta\tau_0) & 4s_0 - 3\Delta\tau_0 & 0 & 2(c_0 - 1) \\ 0 & c_0 & 0 & 0 & s_0 & 0 \\ 0 & 0 & 4 - 3c_0 & 2(1 - c_0) & 0 & s_0 \\ 0 & 0 & 6(c_0 - 1) & 4c_0 - 3 & 0 & -2s_0 \\ 0 & -s_0 & 0 & 0 & c_0 & 0 \\ 0 & 0 & 3s_0 & 2s_0 & 0 & c_0 \end{bmatrix} \tag{3}$$

Traditionally, the linearized equations of motion for orbital rendezvous assume that the target is in a circular orbit. However, Yamanaka and Ankersen [24], Broucke [25], and others have shown that, even with eccentric target orbits, the relative motion can be expressed in a linear form. As a result, the theory derived in this note is valid for elliptical orbits and other general linear dynamic systems.

III. Detectability Concepts

In this discussion, the reference to a *measurement* alludes to a sensor reading at a particular instant in time. A *measurement profile* represents a continuous function describing all the various individual *measurements* over a specified observation period from $\tau_0 < \tau < \tau_f$. There are three types of line-of-sight (LOS) measurement profiles needed to establish the foundation for deriving optimal maneuvers: the *nominal* LOS measurement profile, the *true* LOS measurement profile, and a *unique* LOS measurement profile.

Let the *nominal* state vector $\bar{\boldsymbol{x}}(\tau) = [\,\bar{\boldsymbol{r}} \quad \bar{\boldsymbol{v}}\,] = [\,\bar{x} \quad \bar{y} \quad \bar{z} \quad \bar{x}' \quad \bar{y}' \quad \bar{z}'\,]$ be defined as the relative position and velocity of the chaser spacecraft relative to the target when the acceleration term in Eq. (2) is zero. Consequently, the nominal LOS angle measurement at any given time τ or its continuous profile $\bar{\boldsymbol{i}}_r(\tau)$ over the time interval $[\,\tau_0 \quad \tau_f\,]$ can be written as

$$\bar{\boldsymbol{i}}_r(\tau) = \frac{\bar{\boldsymbol{r}}(\tau)}{|\bar{\boldsymbol{r}}(\tau)|} = \frac{\boldsymbol{\Phi}_{rr}\boldsymbol{r}_0 + \boldsymbol{\Phi}_{rv}\boldsymbol{v}_0}{|\boldsymbol{\Phi}_{rr}\boldsymbol{r}_0 + \boldsymbol{\Phi}_{rv}\boldsymbol{v}_0|} \tag{4}$$

The *true* or *actual* state vector $\boldsymbol{x}(\tau) = [\,\boldsymbol{r} \quad \boldsymbol{v}\,] = [\,x \quad y \quad z \quad x' \quad y' \quad z'\,]$ is defined as the relative position and velocity of the chaser spacecraft relative to the target when the acceleration in the linearized dynamic model [Eq. (2)] is nonzero. In this case, the true LOS angle measurement at any given time τ or its continuous profile $\boldsymbol{i}_r(\tau)$ over the time interval $[\,\tau_0 \quad \tau_f\,]$ can be written as

$$\boldsymbol{i}_r(\tau) = \frac{\bar{\boldsymbol{r}}(\tau) + \delta\boldsymbol{r}(\tau)}{|\bar{\boldsymbol{r}}(\tau) + \delta\boldsymbol{r}(\tau)|} = \frac{\boldsymbol{\Phi}_{rr}\boldsymbol{r}_0 + \boldsymbol{\Phi}_{rv}\boldsymbol{v}_0 + \int_{\tau_0}^{\tau} \boldsymbol{\Phi}_{rv}(\tau,\mu)\boldsymbol{a}(\mu)\mathrm{d}\mu}{|\boldsymbol{\Phi}_{rr}\boldsymbol{r}_0 + \boldsymbol{\Phi}_{rv}\boldsymbol{v}_0 + \int_{\tau_0}^{\tau} \boldsymbol{\Phi}_{rv}(\tau,\mu)\boldsymbol{a}(\mu)\mathrm{d}\mu|} \tag{5}$$

where $\delta\boldsymbol{r}(\tau)$ represents the additional change or *deviation* in the nominal relative position due to the acceleration of the chaser vehicle:

$$\delta\boldsymbol{r}(\tau) = \int_{\tau_0}^{\tau} \boldsymbol{\Phi}_{rv}(\tau,\mu)\boldsymbol{a}(\mu)\,\mathrm{d}\mu \tag{6}$$

A unique LOS measurement profile is one for which, during a given observation period, there is no other possible set of initial position and velocity vectors that could generate the same angular measurements at each and every time instant. For different relative trajectories, there may be intermittent measurements with the same azimuth and elevation readings, but for the entire process the overall measurement profile must be unique. If a measurement profile is unique, this implies that no other combination of initial position and velocity vectors could generate the same observed measurement profile. Under such conditions, the system is considered observable because the initial conditions can be determined uniquely from the measured azimuth and elevation angles. The necessary and sufficient conditions that ensure measurement uniqueness, and therefore observability, are given in [20–22]. Essentially, when a calibrated maneuver alters the natural measurement profile, the amount of angular change θ between the *nominal* and *true* angle measurements is directly related to the initial range and will be referred to as the observability angle. If the observability angle is nonzero at some point during the observation period, then the relative position and velocity are observable. If the observability angle is zero when angle measurements are monitored, then the relative states are unobservable.

IV. Detectability Criteria

Generally observability is treated like a light switch. Either a system is observable or it is not. However, there are several examples in the literature that address the notion that there are *levels* or *degrees* of observability [5,26,27]. Analytically characterizing the degree of observability naturally emerges from the closed-form observability criteria with a metric called *detectability range error*. This metric provides a means to determine how observable the relative states become due to various types of *maneuvers* and, ultimately, becomes the basis for finding optimal maneuvers that maximize observability for angles-only navigation.

The first step in formulating the degree of observability or detectability is to define two critical angles: the observability angle θ and the perturbation angle γ. As depicted in Fig. 1a, the observability angle θ is the angle between the nominal LOS profile $\bar{\boldsymbol{i}}_r$ and the actual LOS profile $\boldsymbol{i}_r$, whereas the perturbation angle γ is the angle between the nominal LOS profile and the perturbation in the relative position due to the maneuver $\delta\mathbf{r}$:

$$\theta = \cos^{-1}(\bar{\boldsymbol{i}}_r \cdot \boldsymbol{i}_r) \qquad \gamma = \cos^{-1}\left(-\bar{\boldsymbol{i}}_r \cdot \frac{\delta\boldsymbol{r}}{|\delta\boldsymbol{r}|}\right) \tag{7}$$

With a known acceleration, the perturbation angle γ in Eq. (7) can be computed. Then, using the law of sines and assuming a perfect angle measurement, the initially unknown range parameter $\rho = |\bar{\boldsymbol{r}}|$ can be uniquely determined:

$$\rho = \delta r\left[\frac{\sin(\theta+\gamma)}{\sin(\theta)}\right] \tag{8}$$

These equations are valid for any arbitrary three-dimensional trajectory.

A. Geometrical Derivation

Now suppose the LOS angle can only be measured to an accuracy of ϵ, as depicted in Fig. 1b, and the trajectory perturbation due to a

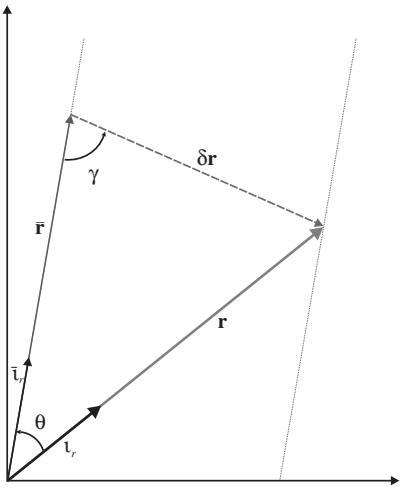

a) *Basic parameters:* the thin solid line represents the nominal trajectory profile *r*, the thick light line is the actual relative position *r*, and the dashed line signifies the perturbation of the trajectory due to maneuvers $\delta\boldsymbol{r}$

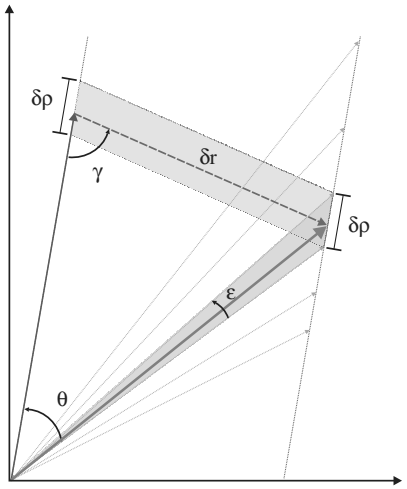

b) *Detectability range error:* the light gray lines represent possible angle measurements while the shaded triangular area depicts the angle accuracy and the shaded rectangular area defines the associated range of detectability

Fig. 1 Angles-only detectability geometry.

maneuver δr is still known perfectly. As a result, there is an inherent uncertainty in the relative range, called the detectability range error metric or $\delta\rho$. Depending on the resulting geometry of the problem, the detectability range error metric $\delta\rho$ varies according to the observability angle θ, the perturbation angle γ, and the sensor accuracy ϵ:

$$\delta\rho = \delta r\left[\frac{2\sin(\gamma)\cos(\epsilon/2)\sin(\epsilon/2)}{\sin^2(\theta)-\sin^2(\epsilon/2)}\right] \tag{9}$$

If the measurement errors are small, the detectability metric can be simplified to a form that is proportional to the measurement error:

$$\delta\rho \approx \epsilon\left[\frac{\delta r\sin(\gamma)}{\sin^2(\theta)}\right] \tag{10}$$

The key factors related to the degree of observability become more apparent by simplifying Eq. (10) in the following compact expression, noting that $\sin(\gamma) = r[\frac{\sin(\theta)}{\delta r}]$ from the law of sines:

$$\delta\rho \approx \epsilon\left[\frac{r}{\sin(\theta)}\right] \tag{11}$$

Knowing the accuracy of the angle measurement, the expected errors in estimating the relative range can be determined for a particular trajectory. Alternatively, if a specific requirement is given for the desired relative range accuracy, the necessary limits on sensor quality can be obtained.

B. Analytical Derivation

Although this derivation is both simple and intuitive, an alternate derivation based on the range error variance is warranted. Assume that a very accurate sequence of azimuth and elevation angle measurements is taken before a maneuver at τ_0; then the relative position and velocity at τ_0 can be determined [20,21] to within a single unknown scalar ρ_0, $\hat{\boldsymbol{x}}_0 = \rho_0\boldsymbol{x}_0$. As a result, the nominal LOS measurement $\bar{\boldsymbol{i}}_r(\tau)$ at any time $\tau > \tau_0$ can then be determined from Eq. (4). If a known maneuver is executed at τ_0, the trajectory deviation $\delta\mathbf{r}$ and γ are also known at any time $\tau > \tau_0$ and can be determined from Eqs. (6) and (7).

Because the observability angle θ is a function of the actual LOS measurement $\boldsymbol{i}_r$ and the known nominal LOS measurement $\bar{\boldsymbol{i}}_r$, it can be defined as an *effective* measurement. Using Eq. (8), the effective measurement $\tilde{\theta}$ can be expressed as a function of the unknown range parameter ρ, the known values of $\delta\mathbf{r}$ and γ, and a small effective measurement error ϵ:

$$\tilde{\theta} = \theta(\rho, \delta\mathbf{r}, \gamma) + \epsilon \tag{12}$$

If the a priori estimate of this measurement is given by

$$\hat{\theta} = \theta(\hat{\rho}, \delta\mathbf{r}, \gamma) \tag{13}$$

the measurement variation, $\delta\tilde{\theta} = \tilde{\theta} - \hat{\theta}$, can be expanded in a Taylor series and expressed to the first order as

$$\delta\tilde{\theta} \approx H(\hat{\theta}, \delta\mathbf{r}, \gamma)\delta\rho + \epsilon \tag{14}$$

where $\delta\rho = \hat{\rho} - \rho$. The effective measurement partial H evaluated at the estimated state then becomes

$$H = \left.\frac{\partial\theta}{\partial\rho}\right|_{\hat{x}} = \frac{-\sin^2(\hat{\theta})}{\delta r\sin(\gamma)} \tag{15}$$

Using this linearized measurement equation, the new range estimate is simply

$$\hat{\rho}^+ = \hat{\rho} + \delta\tilde{\theta}/H \tag{16}$$

and the variance of the range error is simply

$$\sigma_\rho^2 = \epsilon^2/H^2 = \epsilon^2\left[\frac{\delta r\sin(\gamma)}{\sin^2(\hat{\theta})}\right]^2 \tag{17}$$

which is comparable to the previous results derived in Eq. (10). By substituting the identity that $\sin(\gamma) = \hat{r}[\frac{\sin(\hat{\theta})}{\delta r}]$, the standard deviation of the range error becomes

$$\sigma_\rho = \epsilon\left[\frac{\hat{r}}{\sin(\hat{\theta})}\right] \tag{18}$$

consistent with the detectability criteria in Eq. (11).

V. Optimal Observability Maneuvers

The detectability range error $\delta\rho$ in Eq. (11) [see also Eq. (18)] characterizes how accurate the relative range can be determined as a function of the angular measurement uncertainty ϵ, the observability angle θ, and the relative range r. According to this analytical expression, the unknown range parameter can be minimized in three ways. First, obtain a more accurate sensing device to reduce the overall measurement error ϵ. Second, perturb the nominal relative trajectory to generate an observability angle θ near ± 90 deg. Third, maneuver the chaser spacecraft closer to the target to reduce the relative range r.

A simple and practical metric to gauge optimality is to execute maneuvers that minimize the relative range variance such that the cost function J equals

$$J = \left[\frac{r}{\sin(\theta)}\right]^2 \tag{19}$$

By minimizing J, the optimal maneuver will provide the proper balance between causing the observability angle θ to approach ± 90 deg while reducing the relative range required to minimize the uncertainty in the detectability range error $\delta\rho$. This optimization strategy finds the maneuver sequence that alters the relative trajectory to provide the *best* viewing conditions to resolve the only remaining unknown state: the relative range. In other words, it determines the acceleration profile that places the chaser vehicle at the best vantage point to observe the relative states.

A. Optimal Observability Maneuver Analysis

The primary objective of the subsequent analysis is twofold. First, demonstrate how to derive optimal orbital rendezvous maneuvers for angles-only navigation based on the closed-form observability criteria. Second, validate the analytical results using other common navigation methods. For this discussion, an orbital rendezvous scenario is analyzed that assumes the chaser is station keeping in front of the target on the V-bar. This simple yet practical example highlights the fundamental concepts associated with deriving optimal maneuvers.

For the optimal observability analysis, three different techniques are employed. The first approach uses the detectability criteria to analytically derive the optimal maneuver given practical mission constraints. The second method numerically computes the observability angle θ and the detectability range error $\delta\rho$ for a variety of potential maneuvers to confirm the analytical optimization results. The third and final analysis technique is the navigation performance of an angles-only Kalman filter to support and validate the derived analytical results.

The performance of the Kalman filter is evaluated using a linear covariance analysis (LinCov) approach. The fundamental LinCov equations are based on the expressions used to propagate and update the state covariance matrix in a Kalman filter. The only error sources considered are a 0.3 mrad (1σ) angular measurement error and the uncertainties associated with the initial position and velocity of both the target and chaser vehicles. It is assumed that azimuth and elevation measurements are available every 10 s. The chaser's inertial position and velocity are assumed to be known very accurately such that the relative state uncertainty is predominantly

due to the target's inertial state error. The standard deviation of the a priori position uncertainty is selected to be 10% of the actual initial range. The velocity error is then computed as the orbital rate times the initial position uncertainty.

B. Reference Mission Scenario

Suppose that a spacecraft is station keeping on the V-bar some positive downrange distance x_0 from the target for which the initial position and velocity vectors $\boldsymbol{r}_0$ and $\boldsymbol{v}_0$ are, simply,

$$\boldsymbol{r}_0 = [\,x_0 \quad 0 \quad 0\,]^T \qquad \boldsymbol{v}_0 = [\,0 \quad 0 \quad 0\,]^T \tag{20}$$

Before the chaser begins its final approach to either rendezvous with the target or initiate a series of close proximity operations, it is desirable to minimize the uncertainty in the relative downrange location. The mission plan calls for a maneuver to improve the observability in the chaser's downrange position. Depending on a variety of factors, each potential maneuver can produce varying levels or degrees of observability. Which maneuver is optimal in minimizing the uncertainty in the relative range estimate?

To limit the scope of the problem, three practical constraints are made on the types of maneuvers that can be executed. First, it must be impulsive with a fixed magnitude. Second, it is assumed that the maneuver can not change the current orbital energy of the chaser such that the chaser will return to its original location with respect to the target after one orbital period. Third, the maneuver can not cause the chaser to intercept the target or pass beyond it. Essentially, the direction of an acceptable impulsive burn must be perpendicular to the chaser's velocity vector such that it does not have a component in the downrange direction,

$$\Delta\boldsymbol{v} = [\,0 \quad \Delta v\cos(\eta) \quad \Delta v\sin(\eta)\,]^T \tag{21}$$

and the magnitude of the instantaneous maneuver in the altitude direction must be less than the quantity $\Delta v\sin(\eta) < x_0/4$ to ensure the chaser remains in front of the target. The only variable that can be manipulated is the maneuver clock angle η, which is defined as the angle between the positive cross-track direction $\boldsymbol{i}_y = [\,0 \quad 1 \quad 0\,]^T$ and the direction of the impulsive velocity vector:

$$\eta = \cos^{-1}(\boldsymbol{i}_y \cdot \boldsymbol{i}_{\Delta v}) \tag{22}$$

Impulsive maneuvers for orbital rendezvous guarantee observability [20–22], but which maneuver clock angle minimizes the uncertainty in the relative range? The remainder of this analysis focuses on answering this basic question.

C. Analytical Optimal Observability Results

With the impulsive maneuver defined in Eq. (21) and the initial conditions specified in Eq. (20), the cost function in Eq. (19) can be evaluated, noting that $\sin(\theta) = \Delta v s_0/r$ for this simple example:

$$J = [r^2/\Delta v s_0]^2 \tag{23}$$

where $r = |\boldsymbol{r}(\tau)| = |\boldsymbol{\Phi}_{rr}\boldsymbol{r}_0 + \boldsymbol{\Phi}_{rv}(\boldsymbol{v}_0 + \Delta\boldsymbol{v})|$ is the true relative position vector. Recall the shorthand notation defined previously where $s_0 = \sin(\Delta\tau_0)$ and $c_0 = \cos(\Delta\tau_0)$, with $\Delta\tau_0$ representing the flight time following the maneuver. Given the initial conditions outlined for the V-bar station-keeping example,

$$\boldsymbol{r}(\tau) = [\,\{x_0 + 2\Delta v(c_0 - 1)\sin(\eta)\} \quad \{\Delta v s_0 \cos\eta\} \quad \{\Delta v s_0 \sin(\eta)\}\,]^T$$

The partial of J in Eq. (23) with respect to the impulsive maneuver angle η provides a constraint for identifying the optimal maneuver angle,

$$\frac{\partial J}{\partial \eta} = \cos(\eta)\left[\frac{-8r^2x}{\Delta v(1+c_0)}\right] = 0 \tag{24}$$

where x is the downrange location of the spacecraft, $x = [x_0 + 2\Delta v(c_0 - 1)\sin(\eta)]$. Because the maneuver is constrained to keep the chaser in front of the target ($x > 0$), the ratio in Eq. (24) is negative unless it becomes undefined when the flight time is a multiple of a half-orbital period. For the given scenario with the chaser positioned in *front* of the target on the V-bar, the maneuver angles η that minimize and maximize the cost function are those directed in the positive and negative altitude direction, respectively:

$$\eta_{\min J} = \pi/2 \tag{25}$$

$$\eta_{\max J} = -(\pi/2) \tag{26}$$

When the maneuver angle points radially upward $\eta = \pi/2$, the second partial is greater than zero, indicating the cost function is minimized:

$$\frac{\partial^2 J}{\partial \eta^2} = \left[\frac{8r^2x}{\Delta v(1+c_0)}\right] > 0 \tag{27}$$

In other words, by impulsively thrusting in the positive altitude direction, the spacecraft is positioned such that the observability angle θ and relative distance r provide the best possible viewing conditions to reduce the uncertainty in the relative range. If the maneuver angle points downward $\eta = -(\pi/2)$ while the chaser is station keeping in front of the target, the cost function would be maximized:

$$\frac{\partial^2 J}{\partial \eta^2} = -\left[\frac{8r^2x}{\Delta v(1+c_0)}\right] < 0 \tag{28}$$

This suggests that an impulsive maneuver radially downward generates the worst potential viewing angle and relative distance to observe the unknown relative state given the specified constraints. The optimal fixed impulsive maneuver that maximizes the observability conditions without altering the orbital period of the chaser is in the positive altitude direction when the chaser is station keeping in *front* of the target on the V-bar, regardless of when the measurements are observed.

D. Numerical Optimal Observability Results

To validate the derived analytical results numerically, allow the chaser to be station keeping on the V-bar at a relative distance of $x_0 = 100$ m in front of the target. After one orbital period, a fixed impulsive maneuver is executed that generates 20 m of cross-track motion when oriented in the out-of-plane direction. An orbital period later, the chaser spacecraft returns to its original location on the V-bar and executes another impulsive maneuver to null out any relative motion, causing the chaser to return to its initial V-bar station-keeping trajectory. Because of the symmetry of the problem, maneuver angles such as −90, −45, 0, 45, and 90 deg produce the same results as maneuver angles of −90, −135, 180, 135, and 90 deg, respectively. Consequently, the example runs that are used to show the effects of the direction of the maneuver are sampled from the first range of maneuver angles of η equal to −90, −45, 0, 45, and 90 deg, as illustrated in Fig. 2. The symbols in each plot mark where in the trajectory the observability angle is maximized for each maneuver angle to provide a reference point.

Notice in Fig. 3 that the detectability range error is minimized for the entire trajectory when the impulsive maneuver is directed upward ($\eta = +90$ deg) and that the opposite conditions exist for a downward thrust ($\eta = -90$ deg), as predicted in Eqs. (25) and (26). Geometrically, the reason the optimal maneuver angle is $\eta = 90$ deg can be seen by looking at the resulting trajectories. Whether the maneuver is pointed in the out-of-plane direction, radially upward, or straight down, each will cause the chaser to travel to a maximum offset position of 20 m. The out-of-plane burn will cause the chaser to reach 20 m in the cross- track direction, the impulsive burn upward places the chaser on a trajectory to gain 20 m initially in the positive altitude direction and then 20 m in the negative altitude, and the downward thrust produces an initial altitude mark of 20 m downward

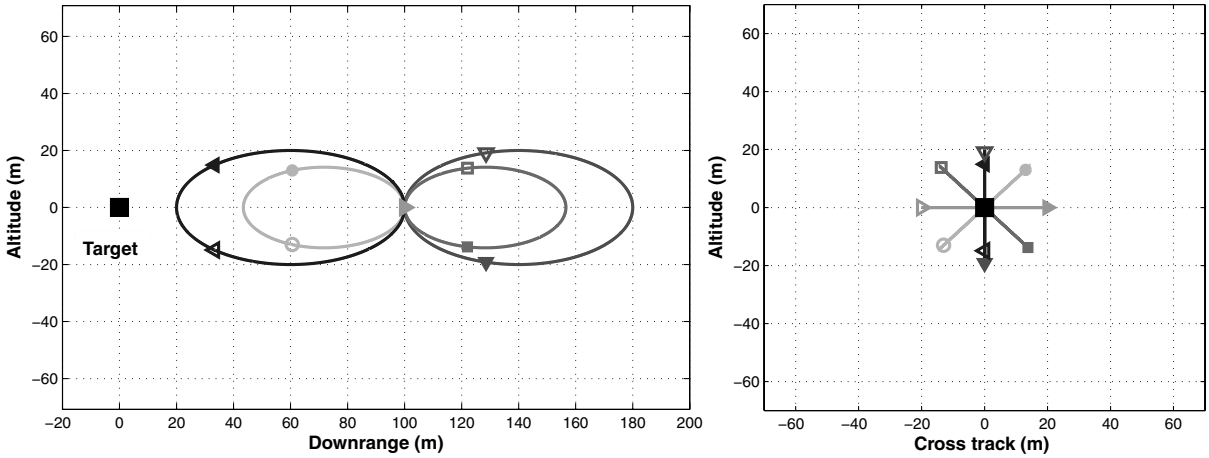

Fig. 2 Resulting relative trajectories for a V-bar station-keeping trajectory with observability maneuver angles η of −90 (down triangle), −45 (square), 0 (right arrow), 45 (circle), and 90 (left triangle) deg. The geometric symbols represent where in the trajectory the observability angle is maximized.

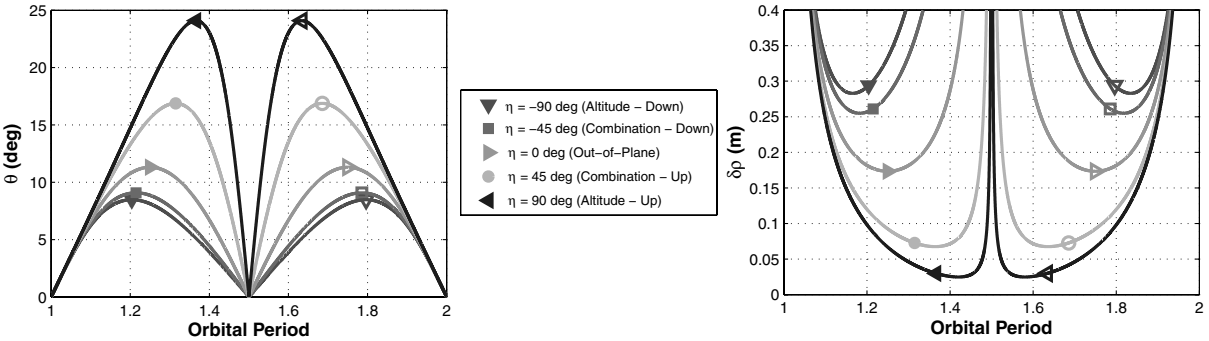

Fig. 3 Observability criteria metrics associated with each maneuver angle. The geometric symbols represent where in the trajectory the observability angle is maximized.

followed by a trajectory that places it 20 m above the V-bar. Clearly, all three eventually generate the same position offset magnitude from the nominal LOS vector. The reason why a maneuver angle of $\eta = 90$ deg maximizes the observability conditions is not only because it generates the maximum observability angle, but also because it reduces the relative distance between the target and chaser. Both the relative distance and the relative position offset generated by the impulsive maneuver ultimately determine the degree of observability and, consequently, the chaser's ability to determine its relative position.

These basic insights for optimal maneuvers derived from the observability criteria are supported by the performance trends of an angles-only navigation filter. In Fig. 4, the linear covariance results for the navigation position errors are plotted for the spectrum of

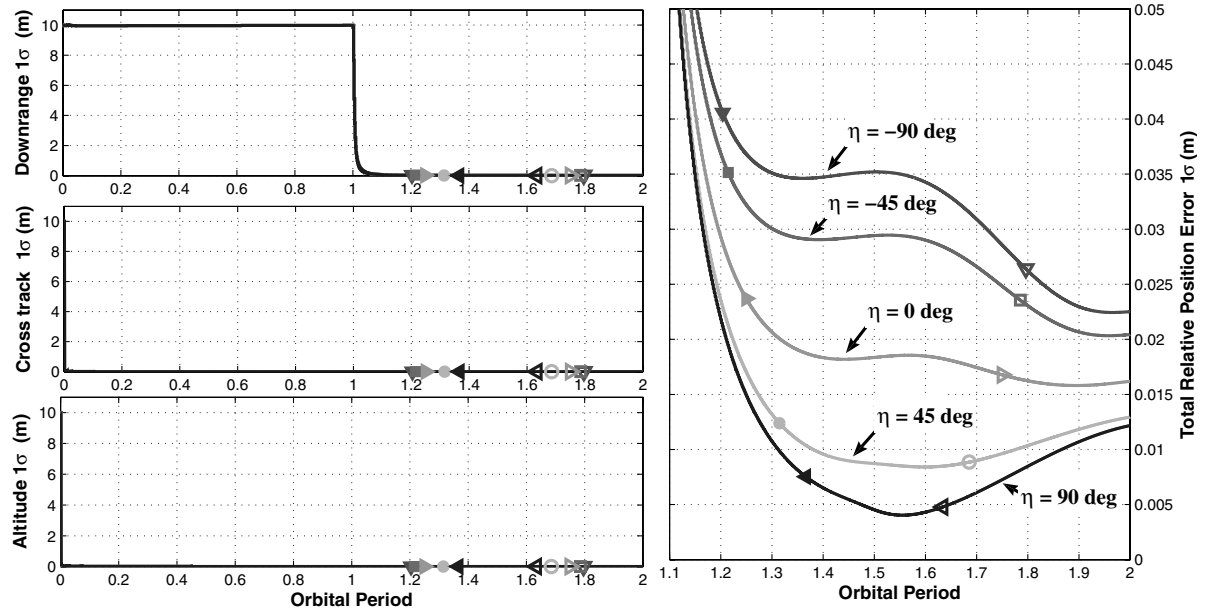

Fig. 4 Resulting relative navigation position errors for a V-bar station-keeping trajectory with observability maneuver angles η of −90 (down triangle), −45 (square), 0 (right arrow), 45 (circle), and 90 (left triangle) deg.

maneuver angles ranging from −90, −45, 0, 45, and 90 deg. Once again, the symbols mark when the observability angle is maximized for each scenario for comparison with the earlier results. From the relative position errors, notice that the uncertainty is minimized for a maneuver angle of 90 deg (left triangle) directed radially upward and maximized with a maneuver angle of −90 deg (down triangle) pointed radially downward. In fact, the overall navigation accuracy for each example follows the pattern anticipated from the numerical observability results. Observability is achieved with each impulsive maneuver, but each maneuver angle generates varying degrees of observability.

VI. Conclusions

Although the capabilities of angles-only navigation to determine the relative range for orbital rendezvous applications are often questioned, it is well understood that strategic maneuvers can eliminate this apparent setback. If properly selected maneuvers produce observability, a very natural question arises as to which ones are *best* in terms of improving the relative state estimate. By refining previously developed closed-form observability criteria for angles-only navigation, this note introduces several important detectability metrics that characterize the *degree* or *level* of observability given noisy angle measurements. With these analytical expressions, it becomes possible to derive optimal maneuvers that produce the *best* possible viewing conditions to observe the unknown relative range parameter. A common orbital rendezvous scenario illustrated the possibility of maximizing the performance of angles-only navigation by deriving optimal maneuvers based on the detectability criteria. Even though this work developed these concepts in the context of orbital rendezvous, they are applicable to general linear dynamic systems and can be extended to nonlinear systems for which LOS angular measurements are used to determine the relative position and velocity.

References

[1] Aidala, V. J., "Kalman Filter Behavior in Bearings-Only Tracking Applications," *IEEE Transactions on Aerospace and Electronic Systems*, Vol. AES-15, No. 1, Jan. 1979, pp. 29–39. doi:10.1109/TAES.1979.308793

[2] Aidala, V. J., and Hammel, S. E., "Utilization of Modified Polar Coordinates for Bearings-Only Tracking," *IEEE Transactions on Automatic Control*, Vol. 28, No. 3, March 1983, pp. 283–294. doi:10.1109/TAC.1983.1103230

[3] Nardone, S. C., and Graham, M. L., "A Closed-Form Solution to Bearings-Only Target Motion Analysis," *IEEE Journal of Oceanic Engineering*, Vol. 22, No. 1, Jan. 1997, pp. 168–178. doi:10.1109/48.557551

[4] Payne, A. N., "Observability Problem for Bearings-Only Tracking," *International Journal of Control*, Vol. 49, No. 3, Aug. 1989, pp. 761–768.

[5] Fogel, E., and Gavish, M., "Nth-Order Dynamics Target Observability From Angle Measurements," *IEEE Transactions on Aerospace and Electronic Systems*, Vol. 24, No. 3, May 1988, pp. 305–308. doi:10.1109/7.192098

[6] Blackman, S., and Popoli, R., *Design and Analysis of Modern Tracking Systems*, Artech House, Norwood, MA, 1999.

[7] Nardone, S. C., and Aidala, V. J., "Observability Criteria for Bearings-Only Target Motion Analysis," *IEEE Transactions on Aerospace and Electronic Systems*, Vol. AES-17, No. 2, March 1981, pp. 162–166. doi:10.1109/TAES.1981.309141

[8] Hepner, S. A. R., and Geering, H. P., "Observability Analysis for Target Maneuver Estimation via Bearing-Only and Bearing-Rate-Only Measurements," *Journal of Guidance, Control, and Dynamics*, Vol. 13, No. 6, Nov.–Dec. 1990, pp. 977–983. doi:10.2514/3.20569

[9] Hammel, S. E., "Optimal Observer Motion for Bearings-Only Localization and Tracking," Ph.D. Thesis, Univ. of Rhode Island, Kingston, RI, 1988.

[10] Hammel, S. E., Liu, P. T., Hilliard, E. J., and Gong, K. F., "Optimal Observer Motion for Localization with Bearing Measurements," *Computers and Mathematics with Applications (1975-) / Computers & Mathematics with Applications*, Vol. 18, Nos. 1–3, 1989, pp. 171–180. doi:10.1016/0898-1221(89)90134-X

[11] Monahan, R. D., "The Optimal Maneuver for Bearings Only Target Tracking," Master's Thesis, Royal Military College of Canada, Kingston, Ontario, Canada, April 1994.

[12] Fawcett, J. A., "Effect of Course Maneuvers on Bearings Only Range Estimation," *IEEE Transactions on Acoustics, Speech, and Signal Processing*, Vol. 36, No. 8, Aug. 1988, pp. 1193–1199. doi:10.1109/29.1648

[13] Helferty, J. P., and Mudgett, D. R., "Optimal Observer Trajectories for Bearings-Only Tracking by Minimizing the Trace of the Cramér-Rao Lower Bound," *Proceedings of the 32nd Conference on Decision and Control*, Vol. WM14-3:10, Dec. 1993, pp. 936–939.

[14] Passerieux, J., and Cappel, D. V., "Optimal Observer Maneuver for Bearings-Only Tracking," *IEEE Transactions on Aerospace and Electronic Systems*, Vol. 34, No. 3, July 1998, pp. 777–788. doi:10.1109/7.705885

[15] Trémois, O., and Cadre, J. L., "Optimal Observer Trajectory in Bearings-Only Tracking for Manoeuvring Sources," *IEE Proceedings Radar, Sonar and Navigation*, Vol. 146, No. 1, Feb. 1999, pp. 31–39. doi:10.1049/ip-rsn:19990262

[16] Oshman, Y., and Davidson, P., "Optimization of Observer Trajectories for Bearings-Only Target Localization," *IEEE Transactions on Aerospace and Electronic Systems*, Vol. 35, No. 3, July 1999, pp. 892–902. doi:10.1109/7.784059

[17] Chari, R. J. V., "Autonomous Orbital Rendezvous Using Angles-Only Navigation," Master's Thesis, Massachusetts Inst. of Technology, Cambridge, MA, May 2001.

[18] Chari, R. J. V., Geller, D. K., Norris, H. L., D'Souza, C. N., and Brand, T. J., "Autonomous Orbital Rendezvous Using Angles-Only Navigation," *AAS/AIAA Astrodynamics Specialists Conference*, Charles Stark Draper Laboratory, Cambridge, MA, Aug. 2001.

[19] Schneider, A. M., Prussing, J. E., and Timin, M. E., "A Manual Method for Space Rendezvous Navigation and Guidance," *Journal of Spacecraft and Rockets*, Vol. 6, No. 9, Sept. 1969, pp. 998–1006. doi:10.2514/3.29746

[20] Woffinden, D. C., and Geller, D. K., "Observability Criteria for Angles-Only Navigation," American Astronautical Society Paper 07-402, 2007

[21] Woffinden, D. C., and Geller, D. K., "Observability Criteria for Angles-Only Navigation," *IEEE Transactions on Aerospace and Electronic Systems*, (to be published).

[22] Woffinden, D. C., "Angles-Only Navigation for Autonomous Orbital Rendezvous," Ph.D. Thesis, Utah State Univ., Logan UT, Sept. 2008.

[23] Clohessy, W. H., and Wiltshire, R., "Terminal Guidance System for Satellite Rendezvous," *Journal of the Aero/Space Sciences*, Vol. 27, 1960, pp. 653–658.

[24] Yamanaka, K., and Ankersen, F., "New State Transition Matrix for Relative Motion on an Arbitrary Elliptical Orbit," *Journal of Guidance, Control, and Dynamics*, Vol. 25, No. 1, Jan.–Feb. 2002, pp. 60–66. doi:10.2514/2.4875

[25] Broucke, R. A., "Solution of the Elliptic Rendezvous Problem with the Time as Independent Variable," *Journal of Guidance, Control, and Dynamics*, Vol. 26, No. 4, July–Aug. 2003, pp. 615–621. doi:10.2514/2.5089

[26] Ham, F. M., and Brown, R. G., "Observability, Eigenvalues, and Kalman Filtering," *IEEE Transactions on Aerospace and Electronic Systems*, Vol. AES-19, No. 2, March 1983, pp. 269–273. doi:10.1109/TAES.1983.309446

[27] Hermann, R., and Krener, A. J., "Nonlinear Controllability and Observability," *IEEE Transactions on Automatic Control*, Vol. 22, No. 5, Oct. 1977, pp. 728–740. doi:10.1109/TAC.1977.1101601